*Refereed Proceedings*

*The 13th International Conference on Fluidization - New Paradigm in Fluidization Engineering*

Engineering Conferences International *Year* 2010

# DIGITAL IMAGE ANALYIS OF BUBBLE FLOW DISTRIBUTION – Influence of operational parameters

Johanna Olsson* David Pallarès†

Filip Johnsson‡

*Chalmers University of Technology, johanna.olsson@chalmers.se

†Chalmers University of Technology

‡Chalmers University of Technology

# DIGITAL IMAGE ANALYIS OF BUBBLE FLOW DISTRIBUTION – Influence of operational parameters

Johanna Olsson, David Pallarès, Filip Johnsson
Department of Energy Technology
Chalmers University of Technology
SE-412 96 Gothenburg (Sweden)

## ABSTRACT

In a first step towards investigating the horizontal fuel mixing in fluidized bed (FB) boilers, this work applies digital image analysis to study the bubble flow properties in a 2-dimensional FB unit. The work investigates the influence of fluidization velocity, bed height and gas-distributor pressure drop on the volume fraction and horizontal distribution of bubbles.

## INTRODUCTION

The performance of large-scale fluidized bed (FB) boilers strongly depends on the fuel mixing and fuel-gas contact. Bubbles govern the in-bed solids (and thereby fuel) mixing pattern and as they erupt at the bed surface they throw solids across the bed surface (1). Solids mixing in FB units is higher in the vertical than in the lateral direction and, thus, the latter being critical for the overall fuel mixing. Important for modeling and scale up of FB boilers is the ratio between the characteristic times for horizontal fuel dispersion and fuel conversion.

Pallarès *et al*. (2) studied fuel mixing patterns in a cold 2-dimensional FB unit, showing that under operational conditions similar to those in FB boilers the fuel flow pattern is structured in horizontally-aligned vortices, as exemplified by Fig. 1a. This pattern is induced by the formation of stable bubble paths through the bed. Thus, there is a clear and strong correlation between the fuel mixing pattern and rate and the bubble flow distribution. This is seen from Fig. 1, where the location of bubble paths identified in Fig. 1b (around x=0.2 and x=1 m) coincides with the symmetry axes of the flow vortices in Fig. 1a for a case run at similar operational conditions. However, there is no correlation available between the horizontal bubble flow distribution and fuel mixing pattern in large scale FB boilers.

Bubble paths are formed by the fact that a bubble, creating a low-pressure path, is followed by other bubbles flowing through the bed. Stable bubble paths have been observed in large-scale FB units and units with low pressure drop distributors (2-4). The formation of bubble paths means that the bubble flow is unevenly distributed in the horizontal direction, as seen in Fig. 1b. Bubble flow properties depend on the operational conditions and in order to be able to improve FB boiler performance it is

important to understand the influence of operational conditions on the bubble flow. FB boilers operate at fluidization velocities far higher than the minimum fluidization velocity and with relatively low gas distributor pressure drops which promotes large bubbles of an exploding type. Such conditions influence the gas flow distribution in the boiler since the gas flow is considerably higher than what corresponds to the visual bubble flow. A significant fraction of the gas flow passes the dense bed as so-called throughflow following the bubble paths (5, 6).

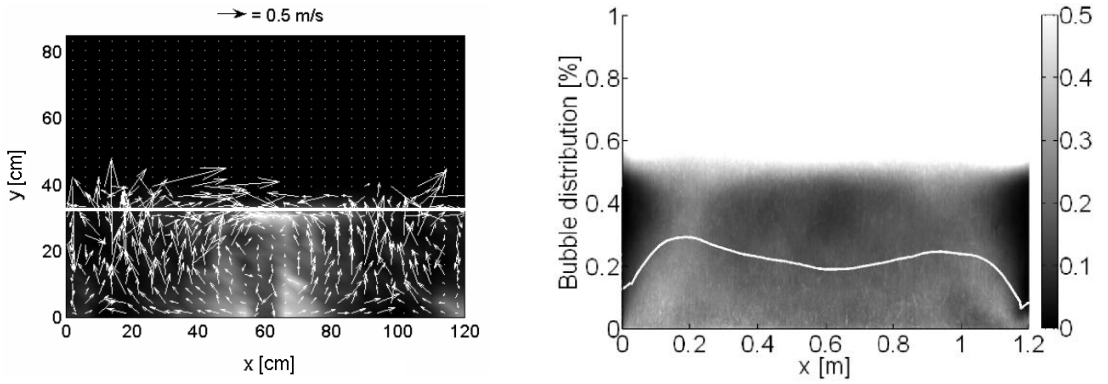


a) Fuel mixing flow pattern. Tracer concentration (gray field) and tracer velocity (vector plot). From Pallarès *et al.* (2) with permission, $H_0$ = 0.33 m, $u$ = 0.7 m/s, $k$ = 1046 Pa*s$^2$/m$^2$.

b) Time-averaged bubble density (gray field) and bubble flow distribution profile (curve). From present work, explanation further down. $H_0$ = 0.4 m, $u$ = 1.0 m/s, $k$ = 1046 Pa*s$^2$/m$^2$.

**Figure 1: Comparison between the fuel mixing flow pattern (17) and the horizontal bubble flow distribution (present work), both indicating preferred bubble paths at about 0.2 and 1 m.**

Lim *et al*. (7) were the first to use Digital Image Analysis (DIA) to study bubble properties in 2-dimensional fluidized beds. This work was followed by other studies which further developed the use of the DIA technique for studies of hydrodynamics and bubble properties in FB units (8-14). DIA allows for studies of both the transient behavior and the spatial distribution of bubble properties. Sequential analysis of video frames reveals fluctuations and distributions of properties which, using other measurement methods can only be measured as time, or space-averaged values. An obvious drawback of DIA is, however, its limitation to 2-dimensional beds. The aim of this work is to apply a DIA method to study the influence of key operational parameters (dense bed height, fluidization velocity and gas distributor pressure drop) on the bubble flow distribution under operating conditions representative for FB boilers.

## THEORY

The modified two-phase flow model (see Johnsson *et al* (5) and references therein) divides the gas flow through the bed into three parts: a minimum fluidization flow which is assumed to flow in the solids emulsion under minimum fluidization conditions, a visible bubble flow and a gas throughflow flowing at a relatively high velocity through and between the bubbles. The last term made it possible to close the gas mass balance. For fluidization velocities much higher than the minimum fluidization velocity, the throughflow becomes the dominant part of the flow. As a result of increasing throughflow, a dense bed can be maintained at fluidization velocities several times that of the terminal velocity of the bed solids (6 and references therein).

Using the fact that the pressure gradient (proportional to the bed voidage, as expressed by Eq. (1)) in a freely bubbling bed is independent of the vertical position in the bed, a model for the bed expansion was derived by Johnsson *et al* (5). Assuming the emulsion to remain under minimum fluidization conditions, $\varepsilon_{mf}$, the time-averaged bed voidage, $\varepsilon_b$, is calculated as the weighted sum of the voidage in the two phases, as expressed by Eq. (2).

$$-\frac{dp}{dh} = \rho_s(1-\varepsilon_b)g \qquad (1)$$

$$\varepsilon_b = (1-\delta_b)\,\varepsilon_{mf} + \delta_b \qquad (2)$$

where $\delta_b$ is the time-average bubble fraction

## EXPERIMENTS

The DIA method was applied to a 2-dimensional cold fluidized bed with a transparent front wall, schematized in Fig. 2. The riser is 1.2 m wide with a depth of 0.02 m and a height of 2.05 m. The front wall is made of Plexiglas, allowing visual observations of the bubble flow. The bed was illuminated from the front with four halogen lights (300 W). The bed particles were glass beads with a narrow particle size distribution with an average particles size of 330 µm and a density of 2 500 kg/m$^3$, both similar to those of bed material in boilers. The particles belong to group B in the Geldart classification with a minimum fluidization velocity of 0.12 m/s and terminal velocity of 1.76 m/s (ambient conditions). The two gas distributors used in the experiments are perforated plates, both with 2 mm I.D. holes and total hole fraction of 2% and 9%, respectively, yielding the pressure drop curves shown in Fig. 3 ($\Delta p_{dist} = k \cdot u^2$) with pressure constants $k$ of 50 and 1 046 (Pa*s$^2$)/m$^2$, respectively. The gas distributors are covered by a fine mesh net to avoid bed material to fall down into the air plenum when bed is not in operation.

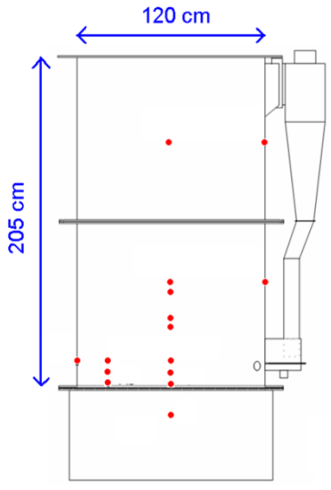


**Figure 2: The cold 2-D FB unit used in the experiment. Pressure taps marked with dots**

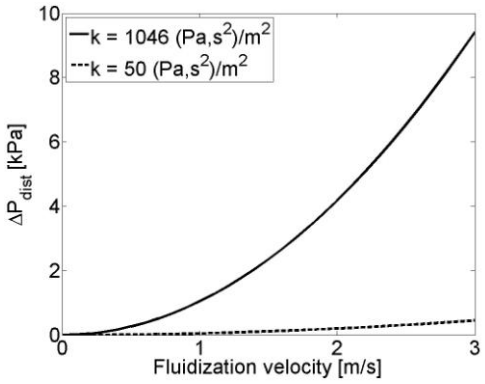


**Figure 3: $\Delta p$-$u$ curves for the gas distributors used in the experiments**

The visible bubble flow was recorded during 2 minutes with a digital SLR camera (Nikon D90) with a time resolution of 0.04 s, yielding statistically reliable results. To increase the contrast between the emulsion and the bubble phase, the rear wall of the bed is coated with a black film which can be seen when bubbles span across the depth

of the bed. The test matrix and operational conditions used in the experiments (given in Table 1) consisted of five levels of fixed bed height, corresponding to that of the static non-fluidized bed, $H_0$, seven different fluidizing velocities, $u$, and the two above-mentioned gas distributors.

The entrance of the particle recirculation duct was found to have no significant influence on the bubble flow distribution. This, since measurements under bubbling conditions with and without the entrance of the recirculation duct blocked, gave similar results. Minor solids inventory losses through the cyclone during operation under circulating conditions were detected but are considered negligible compared to the total bed inventory and not to have any significant influence on the results shown here.

**Table 1: Operational conditions during experiments**

| | | |
|---|---|---|
| Particle size, $d_p$ | 330 | µm |
| Particles density, $\rho_s$ | 2 500 | kg/m$^3$ |
| Fluidizing medium | Air at 298 K | |
| Fluidizing gas velocity, $u$ | 0.5, 0.75, 1.0, 1.5, 2.0, 2.5, 3.0 | m/s |
| Fixed bed height, $H_0$ | 0.2, 0.3, 0.4, 0.5, 0.6 | m |
| Distributor constant, $k$ | 50, 1 046 | Pa,s$^2$/m$^2$ |

## THE DIGITAL IMAGE ANALYSIS

Digital Image Analysis (DIA) requires the images, *i.e.* video frames, from the SLR camera to be of gray-scale type. Thus, color images are transformed into gray-scale images prior to the DIA. The principle of the DIA is to use the pixel intensity to discriminate between bubble and emulsion phases (13). Thus, if the pixel intensity is below a certain threshold value, the pixel area is assigned to the bubble phase and otherwise to the emulsion phase.

Bubbles extending across the entire depth of the bed are easily detected due to that these will give rise to high contrast between the emulsion and the black rear-wall. Rapid moving bubbles with bed material raining from the bubble roof and bubbles not spanning across the entire depth of the bed give a lower contrast and are therefore more difficult to detect. While a too low threshold value will not detect all bubbles present in the image, a too high value will result in emulsion pixels erroneously considered as being part of the bubble phase. Hence, the selection of an appropriate threshold is crucial for the analysis and different methods for automatic selection of a threshold value have been proposed by e.g. Otsu (16) and Kapur *et al*. (17). The most commonly used methods are based on the gray-scale histogram of the image. However, this approach is not feasible in unevenly illuminated images with a low contrast, which was the case for the experiments in this work (due to blurring effects from rapid movements in the bed as well as uneven illumination)

In this work, the discrimination of pixels is based on a double threshold method; with one (lower) value to determine the dense bed surface and one (higher) value to detect the bubbles in the bed. The maximum intensity in a pixel is obtained when that point is occupied by emulsion and, thus, values below this maximum indicate increased voidage. The threshold for the individual pixel is selected as the maximum value pixel obtained during the video recording multiplied by one factor for each of the two thresholds used. In this work, threshold values are selected in such a way that the

bubble fraction resulting from DIA matches that calculated from pressure measurements. Thresholding a gray-scale image results in a binary image, as exemplified in Fig. 4a. Thus, sequences of such binary images are used to calculate the bubble flow properties, e.g. the average bubble density in Fig. 4b.

The averaged bubble fraction in each frame is determined as the fraction of bed pixel area appointed as bubble phase, according to Eq. (3). The time-averaged bubble fraction is obtained by averaging the bubble fraction obtained with Eq. (3) over the video recording. The horizontal bubble distribution profile is calculated according to Eq. (4) as the ratio of bubble pixel area along each x-coordinate compared to the total amount of bubble pixel area. This value is averaged throughout all frames in the video recording. The evenness of the horizontal bubble distribution is evaluated with the variance of the profile obtained, according to Eq. (5).

$$\delta_b = \overline{\left(\frac{\sum_{J=1}^{N} A_J}{A_I - A_{FB}}\right)} \qquad (3)$$

$$P|_x = \frac{\sum_{j=1}^{N} A_j|_x}{A_{Tot}} \qquad (4)$$

$$\sigma^2 = \frac{1}{X}\sum_{i=1}^{X}(P_i - \bar{P})^2 \qquad (5)$$

where

| | |
|---|---|
| $A_j$ | = bubble pixel area |
| $A_I$ | = pixel area in frame |
| $A_{FB}$ | = pixel area of freeboard |
| $N$ | = no of bubbles in frame |
| $A_{Tot}$ | = total bubble pixel |
| $P$ | = fraction of bubble pixels |
| $X$ | = no of x-coordinates |
| $\sigma^2$ | = variance of P |
| $\bar{P}$ | = average value of P |


a) Binary image b) Time-averaged bubble density

**Figure 4: Images derived through DIA, operational conditions: High ∆p-plate, $H_0$ = 0.4m, $u$ = 1.0m/s**

## RESULTS AND DISCUSSION

Figure 5a shows the time-averaged bed voidage as obtained from pressure measurements from the centre-line pressure taps (*cf.* Fig. 2) using Eqs (1) and (2). The obtained bed voidages values are similar to corresponding measurements available in literature (5, 6, and references therein). Svensson *et al*. (6) report lower bed voidage for distributors with lower pressure drop but this effect disappears for gas velocities above 1.8 m/s. As shown in Figure 5b, the present work also shows an influence of the gas-distributor pressure drop at low velocities, but this vanishes as velocity increases above 1 m/s, most likely due to that the velocity is sufficient to make the voidage

independent of distributor pressure drop. In contrast to the results of Svensson *et al*. (6) the average bed voidage obtained here is higher for lower distributor pressure drop. Figure 5b also shows that the voidage decreases slightly with increasing bed height which is in accordance with the observations made by Svensson *et al*. (6).

It must be noted that for the lower bed heights (0.2 and 0.3 m) applied in this study, there are only three pressure taps within the dense bed with the upper pressure tap located around the dense bed surface. Thus, the calculated average voidage values are based on only two pressure points, *i.e.* making it somewhat less reliable.

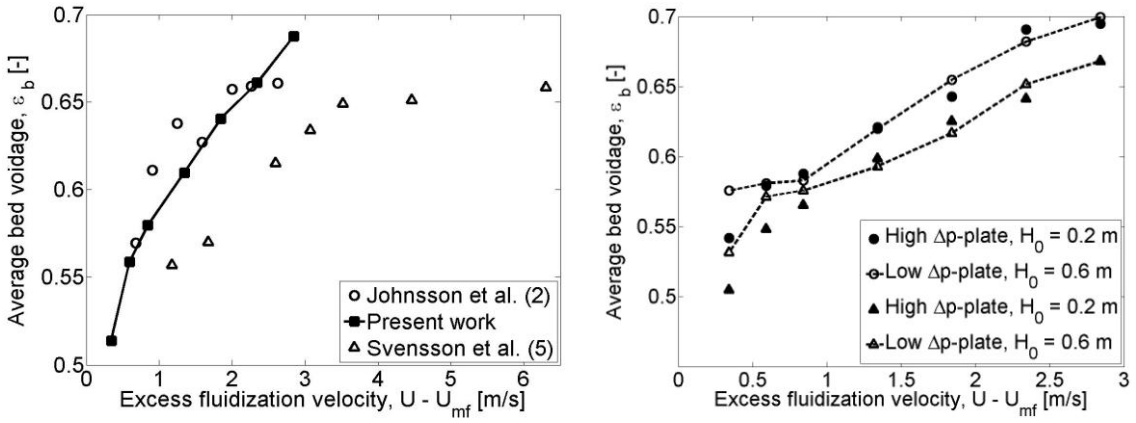


a) Values from present work (solid line with markers) and from literature.

b) Bed voidage from this work for two different bed heights and distributor plates.

**Figure 5: Time-averaged bed voidage as a function of excess gas velocity.**

Figure 6 shows the horizontal bubble distribution profile obtained through the DIA for four different sets of operational parameters. A reference case ($H_0$ = 0.2 m, $u$ = 0.75 m/s and $k$ = 50 Pa*s$^2$/m$^2$) is compared with cases in which one of the operational parameters is increased: increased bed height (0.6 m), increased gas velocity (3.0 m/s) and increased gas distributor pressure drop (1 046 Pa*s$^2$/m$^2$). If the pressure drop across the distributor or the fluidizing gas velocity is increased, the bubble distribution evens out. The opposite effect is obtained if the bed height is increased (at constant velocity).

Figure 7 shows the variance of the horizontal bubble distribution profile as a function of fluidization velocity. It can be seen that the variance decreases with gas velocity, increases with bed height and, to a smaller extent, decreases with increasing gas distributor pressure drop. A low variance indicate an even bubble distribution but a low variance alone is no guarantee that the entire bed is fluidized properly. For any combination of dense bed height and gas distributor plate there is a certain gas velocity above which the horizontal bubble distribution becomes even.

Uneven bubble distributions were obtained at low gas velocities, regardless of distributor and bed height (not shown here), *i.e.*, at low velocities, none of the plates provides a pressure drop high enough to ensure an even bubble distribution, not even for the lowest bed height. Hence, if the gas distributor pressure drop is low, which is common in industrial boilers, and the aspect ratio of the bed is low enough not allowing single bubbles to grow so that they occupy the entire width of the bed, then the bubble

flow distribution is uneven at low velocities. For high gas velocity the gas distributor pressure drop increases and the bubble distribution evens out. Thus the impact the presence of a bubble has on the gas flow depends on the relative pressure drop across the distributor plate and the bed.

If the relative pressure drop across the distributor increases, then the horizontal bubble distribution evens out. Decreasing the relative pressure drop across the distributor, promotes an uneven bubble distribution. Hence, the horizontal bubble distribution depends, as can be seen in both Fig. 6 and 7, on all the investigated key parameters. The gas velocity required to obtain an even fluidization of a given bed height is higher than for a distributor providing a higher pressure drop, see Fig. 7. This is especially critical for CFB boilers operating at part load (and thereby at fluidization velocities below the design point). Due to operational costs, the gas distributor pressure drop is often kept as low as possible.

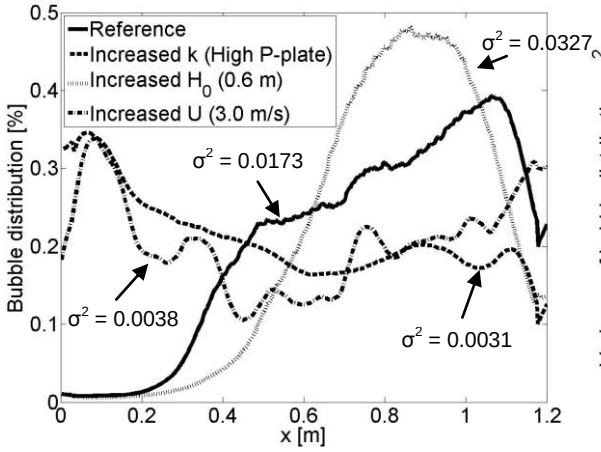


**Figure 6: Bubble distribution profile as obtained from DIA. Reference conditions: Low $\Delta p$-plate, $H_0$ = 0.2 m and $u$ = 0.75 m/s.**

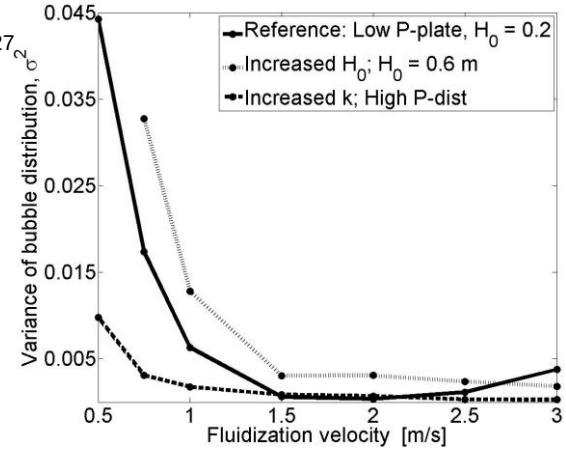


**Figure 7: Variance of bubble distribution as a function of fluidization velocity. Reference conditions: Low $\Delta p$-plate and $H_0$ = 0.2 m.**

Pallarès *et al*. (2) reported that the fuel mixing rate, *i.e.* dispersion rate, is enhanced by increased gas velocities and increased bed heights (at constant velocity). In this work it is shown that the variance of the horizontal bubble distribution is decreased by increasing gas velocities but that for low velocities, increasing bed heights makes the bubble distribution less even. This difference can be due to that a high gas velocity (2.7 m/s) and shallow beds (0.18 m and 0.33 m) were employed and, therefore, the bubble flow distribution is fairly even for both bed heights investigated by Pallarès *et al*..

Pallarès *et al*. (2) also report that lowering the distributor pressure drop (at constant velocity, 2.7 m/s, and bed height, 0.18 m) significantly reduces the solids mixing, which according to the results in this work should be a result from an uneven bubble distribution. Correlating the results for the horizontal bubble distribution from this work to those obtained for fuel mixing patterns by Pallarès *et al*. further support the hypothesis that the horizontal bubble distribution is of significant importance for fuel mixing in FB boilers, see Fig. 1.

## CONCLUSIONS

A digital image analysis (DIA) method has been used to study the horizontal bubble flow distribution in a 2D fluidized bed. The method is based on adjusting the threshold value in order to match the voidage resulting from the DIA analysis to that calculated from pressure measurements.

As expected, the horizontal distribution of the bubble flow becomes more even as gas velocity increases, bed height is lowered and gas-distributor pressure drop is increased. The velocity required to obtain an even horizontal bubble distribution is determined by the ratio between the pressure drop across the distributor and the bed and for any combination of dense bed height and gas distributor plate there is a certain gas velocity above which the horizontal bubble distribution becomes even. Correlating the results from this work to those of Pallarès *et al*. (2) enhances the importance of the bubble flow distribution for the fuel dispersion.

## ACKNOWLOGMENTS

The authors gratefully acknowledge financial support from the Waste Refinery project.

## REFERENCES

[1] Yan F.S., Fan L.T., (1984), *Ind. Chem. Process Des. Dev.*, 23, 337-341
[2] Pallarès D., Díez P.A., Johnsson F., (2007), *Proc. Of the 12th Int. Conf. on Fluidization*, 929-936
[3] Pallarès D., Johnsson F., (2006), *Chem. Eng. Sci.*, 61, 2710-2720 Lim C.N., Gilbertson, M.A., Harrison A.J.L., (2007), *Chem. Eng. Sci.*, 62, 56-69
[4] Werther J., (1977), *Int. J. Multiphase Flow*, 3(4), 367-381
[5] Johnsson F., Andersson S., Leckner B., (1991), *Powder technol.*, 68, 117-123
[6] Svensson A., Johnsson F., Leckner B., (1996), *Int. J. Multiphase Flow*, 22(6), 1187-1204
[7] Lim K.S., Agarwal P.K., O'Neill B.K., (1990), *Powder technol.*, 60, 159-171
[8] Lim C.N., Gilbertson, M.A., Harrison A.J.L., (2007), *Chem. Eng. Sci.*, 62, 56-69
[9] Agarwall P.K., Hull A.S., Lim K.S. (1996). *Non-Invasive Monitoring of Multiphase Flows*, Chap.12, 407-454
[10] Goldsmidt M.J.V., Link J.M., Mellema S., Kuipers J.A.M., (2003), *Powder technol.*, 138, 135-159
[11] Shen L., Johnsson F., Leckner B., (2004), *Chem. Eng. Sci.*, 59, 2607-2617
[12] Mudde R.F., Schulte H.B.M., van den Akker H.E.A., (1994), *Powder technol.*, 81, 149-159
[13] Laverman J.A., Roghair I., van Sint Annaland M., Kuipers H., (2008), *The Canadian Journal of Chemical Engineering*, 86, 523-535
[14] Caicedo G.R., Marqués J.J.P., Ruíz M.G., Soler J.G., (2003), *Chem. Eng. & Proc.*, 42, 9-14
[15] Otsu N., (1979), *IEEE Transactions on systems, man, and cybernetics*, 9(1)
[16] Kapur J.N., Sahoo P.K., Wong A.K.C., (1985), *Computer vision, graphics, and image processing*, 29, 273-286